BACHELOR THESIS

MECHANICALLY ACTIVATED IN-VITRO MUSCLE MODEL

Mitchel Doets

ENGINEERING TECHNOLOGY - BIOMECHANICAL ENGINEERING
DR.IR. J. ROUWKEMA

EXAMINATION COMMITTEE
C. RIVARES BENITEZ, MSc
PROF.DR. P.C.J.J. PASSIER

DOCUMENT NUMBER
BE - 881

UNIVERSITY OF TWENTE.

JULY 2022

1 Abstract

Spasticity is a common disorder that more than 12 million people on world scale are suffering from. Within this disorder high amounts of contraction stimulus and velocity-depended stretch reflexes are seen, which result in possible shortening or stiffening of the muscle. It was aimed to design an in-vitro system to prove eccentric training as a stimulus for longitudinal muscle growth by sarcomere addition in series, to improve locomotion of patients with spasticity. This goal was aimed to be reached within 11 weeks.

Requirements were formulated to control suitability for the main goal. Six systems were evaluated. A 3D printed prototype was designed and fabricated. Accuracy measurement of the system was performed for steps distances between 10 and 0.1 mm for increasing and decreasing pillar distance. For this measurement, a syringe pump was used with an accuracy of $\pm$ 0.25%. The steps were performed with a speed of 220 µm/s, the movement was tracked by a digital microscope.

It was found that a hydrostatic pressure-driven system using PDMS pillars and a syringe pump was most adequate. This system fits six tissues with a maximal of $2.5 \cdot 10^5$ cells per tissue. It is seen that accuracy decreases by downsizing the step distance, from 86.4 % $\pm$ 0.8 for the steps of 10 mm to 54 % $\pm$ 10 for steps of 0.1 mm. The potential to mechanically stretch tissue by this system was proven by theory.

It can be concluded that the system is up to nine of the eleven set requirements. The system has very high potential to be used to proof eccentric training as stimulus for longitudinal muscle growth.

Contents

2 Introduction

On a world scale, more than 12 million people have or suffer from muscle spasticity [1]. In this disorder more muscle stimulus is found than usual. This involuntary stimulus coming from the upper motor neurons initiates shortening or contraction of the muscle tissue [2]. Due to co-contraction of antagonistic muscles, spasticity can be a major cause of undesirable imbalanced force distribution of the locomotor system [1] resulting in a greater incidence of joint subluxations and dislocations, bony deformities and muscle shortening [1].

Most patients suffer from shortened muscles. This is caused by high amounts of velocity-dependent tonic stretch reflexes. The high amount of contraction stimulus of the muscle enforces an increased elongation resistance, resulting in a possible shortening or stiffening of the muscle. As a result, deformation of the wrist is commonly seen in patients suffering from muscle spasms. Due to maladaptation within childhood, spastic effects can be amplified [3]. That is why patients with muscle spasms are suffering from longer and more stretchable tendons, resulting in a smaller muscle-tendon ratio caused by a smaller amount of sarcomeres build in series than seen in patients within a healthy control population. As result, a smaller muscle length range of motion and active force exertion can be seen in patients with spasticity in comparison to people without spasticity.

Nowadays, Botulinum toxin type A (BoNT-A) injections are the most common treatment used for spasticity. Botulinum toxin prevents the excitation of acetylcholine from the presynaptic-ends, interfering with the normal vesicle-membrane fusion. The effect of Botulinum toxin on muscle tissue can be described as neurological paralysis, the term chemical denervation is also often used for describing the effects of Botulinum toxin [4].

However, experimental animal studies and in-human investigation points out that after the use of Botulinum toxin injections for at least 12 months a decrease in sarcomeres is seen. These sarcomeres are replaced by scar tissue. Also, overall atrophy of the muscle is seen [4].

To overcome these drawbacks this research aims for a non-invasive treatment for spasticity by remediation of shortened muscle. In this thesis, shortened muscle will be defined as a short muscle relative to the normal muscle length that would be expected in rest position for this muscle in a healthy patient without muscle spasticity. This will be formulated as a shortage in the number of sarcomeres in series.

A pennate muscle can also shorten due to a decrease in sarcomeres built in parallel, this can be caused by atrophy. Atrophy is a process where degeneration of overall muscle size is seen, the term hypertrophy is used for an overall muscle size increase [5]. However, this thesis focuses on sarcomeres shortage and addition in series in parallel fibered muscle.

Eccentric training is suggested to be a potential incentive stimulus for muscle hypertrophy [5]. A system that elongates muscle tissue as a function of time and enables active contraction simulation simultaneously has not yet been described in the literature.

The main goal of this research is: 'Creating a model to proof eccentric training as a driver for longitudinal muscle growth to improve locomotion of patients who are suffering from spasticity.' This goal is aimed to be reached within a limited time-span of eleven weeks.

To prove eccentric training as a strategy to induce longitudinal muscle growth in humans, firstly information about muscle composition will be given. Secondly, the key part for longitudinal growth and eccentric training will be considered. Finally, a system will be designed to induce longitudinal growth in human cells.

2.1 Contractile units

Skeletal muscles are part of the striated muscle, characterized by thousands of parallel aligned myofibers, consisting of long series of sarcomeres [6]. The contractibility of the muscle depends on several determinants such as fatigue, stimulation, recruitment and amount of sarcomeres. Taking into account the main goal of this thesis, 'proving eccentric training as a driver for longitudinal growth by addition of sarcomeres in series', this thesis will focus on the sarcomeres as the determinant for contractibility.

Due to action potentials coming from the neuromuscular junction, calcium ions are released by the sarcoplasmic reticulum. This results in troponin changing its configuration on the actin filaments creating a possibility for myosin to bound to actin, starting the contraction cycle. Figure 1 gives an graphical representation of this cycles [7]. The parallel configuration of these actin-myosin interfaces are called sarcomeres and these are the contractile units of a muscle.

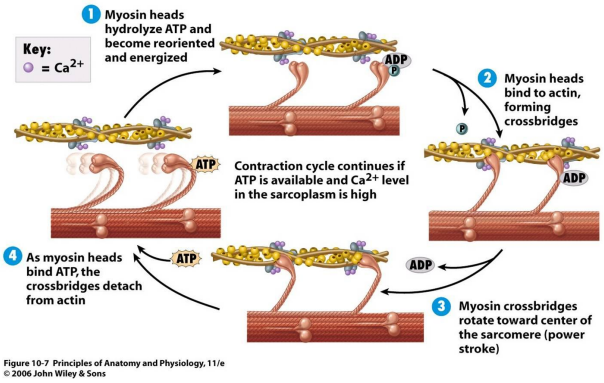

Figure 1: *Schematically representation of muscle contraction on protein level [8]*

The contraction and extension of sarcomeres are limited to a certain range. The theoretical minimum length of sarcomeres in the human gastrocnemius is 1,0 µm and the maximum theoretical length is 4,4 µm [9]. These limitations result in the existence of a muscle length-force relationship limited by maximal sarcomere lengths and number. In this relationship active force is caused by contractions in sarcomeres induced by action potentials. Passive force is caused by the elastic behaviour of muscle elements mostly generated by the protein Titin, but also by sarcomeres in parallel [10]. The elasticity of skeletal muscle can defined with it Young's modulus of 24.7 $\pm$ 3.5 kPa [11]. The muscle length-force relationship is defined based on the active and passive slack lengths, active slack length is the length where there is no active force exerted while being stimulated by the sarcomeres. Passive slack can be defined as a length where no passive force is seen (figure 2).

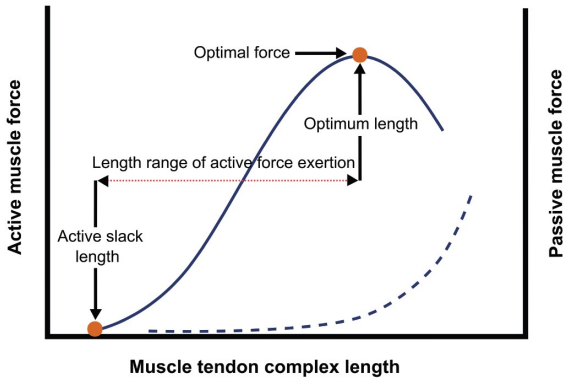

Figure 2: *Graphical representation of the muscle length-force relationship, were the bold line displays active force and the dashed line the passive force. [12]*

2.2 Longitudinal muscle growth

Most human muscles have a pennate orientation, here the myofibers are orientated obliquely to the line of pull of the muscle-tendon complex. The amount of sarcomeres in series in combination with the pennation angle determines the muscle belly length [12] and the length range where muscle force can be generated. To create a longer muscle-tendon complex sarcomerogenesis is needed. In this process individual myofibers elongate. The process originates from the addition of sarcomeres in series at the ends of the myofibers. This results in longitudinal growth of the muscle belly. The myofiber grow-terminals are built oblique to able sarcomere addition without the interference of the mechanical continuity of the muscle. In this process, the protein dystrophin acts as a mechanochemical transducer [13].

2.3 Eccentric training

A training regime where a force is applied on the muscle-tendon complex greater than the contractile force of the complex when stimulated is called eccentric training. This enforces elongation of the muscle while contracting, which should result in sarcomerogenesis [5][14]. Animal studies point out that eccentric training

can induce longitudinal muscle growth by the addition of sarcomeres in series. Human studies do suggest longitudinal growth due to eccentric training but based on methodology these studies cannot be reliable [12]. Due to ethical considerations, extracting a human muscle and performing direct research on it is not allowed.

To prove longitudinal growth in human muscle by serial sarcomere addition resulting from eccentric training an in-vitro model is needed. In this thesis, an in-vitro model will be designed. The in-vitro system will be tested on performance by measuring the deviation between the set mechanical action and the actual performed action.

If eccentric training is a stimulus for the addition of sarcomeres in series then a shift towards a longer working length in the length-force relation should be seen.

3 Requirements

A system that facilitates human cell-culturing, can stimulate the cells and is manufacturable demands very specific requirements. To supply/replace cell culture media or to let air escape from the system an in- and outlet are needed. To create a proper environment for the cells the system should be biocompatible and sterile. Furthermore, to prove that the system is suitable for fulfilling the main goal as stated in chapter 2, the system should be measurable. This can be formulated by the following requirements:

1. The system should be possible to keep sterile.
2. The system should be bio-compatible with human cells.
3. The system should contain the possibility to refresh or add media to the cells.
4. The system should provide enough space to culture a tissue with a cross-sectional area of 100-200 micron.
5. The system should contain a device that can induce mechanical stimulation in the longitudinal direction.
6. The system should contain the possibility to pace the cells by electronic stimulation.
7. The force generated by the tissue cultured in the system should be determinable.
8. The length of the tissue-cultured on the system should be measurable.
9. The system has to be able to elongate the tissue by a minimum of 20% of the initial tissue length.
10. The performed step of the system, initiated by the set elongation of the system should have an accuracy of a minimal of 90% compared to the set step.
11. The system should allow fluorescence-microscopic investigation of the tissue.

4 System and concept evaluation

In this section, a selection of pre-existing and concept in-vitro systems will be evaluated, and the characteristics of these systems will be used for the design considerations of a prototype. The first two described systems are pre-existing and already commercially available. The remaining concepts are designed within this research. An assessment of the suitability of the systems for this research will be made.

4.1 Biomimx - uBeat®

This commercially available system consists of a cell platform where tissues can be cultured. The uBeat can simulate the stretching movement of the tissues, making use of pressure and a flexible membrane (Figure 3). It can induce a maximal deformation of 10% in the length direction [15]. The main advantage of this system is the already proven workability and availability. A major drawback of this solution would be that fixation of the tissue is needed, without fixation the tissue would be compressed instead of elongated. However, fixation of the tissue is not possible within this system. Besides, tension measurement of the tissue within this system cannot be performed. Nevertheless, requirement 9 as described in the system requirements (Chapter 3) cannot be satisfied without adaption of the system.

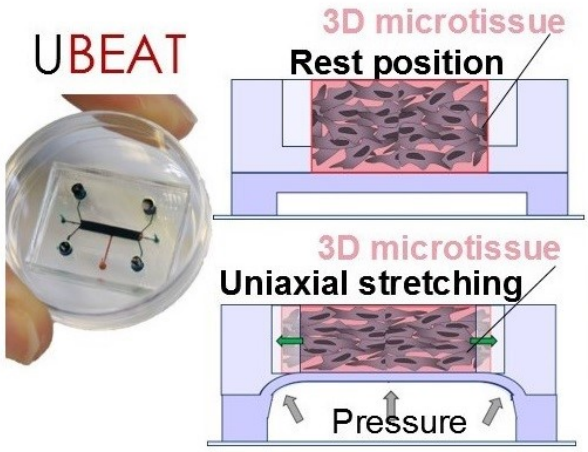

Figure 3: *Schematically representation of the Biomimx - uBeat® system [16]*

4.2 Biowire™ II Platform

The Biowire system is also commercially available and makes use of two wires where the tissue is spun between. When the wires are tensioned, mechanical stimulation of the tissue can be performed in a longitudinal direction (Figure 4). To have a large extension reach to be able to train eccentric, the tissue should be cultured around the wires. The wires should be placed in the most relaxed position facing each other. The smaller the distance between the attachment sites of the wires in starting position, the greater the extension reach. Culturing cells in this relaxed wire position could be very complex [17]. This system is proven to be workable but is not easily applicable in combination with eccentric training.

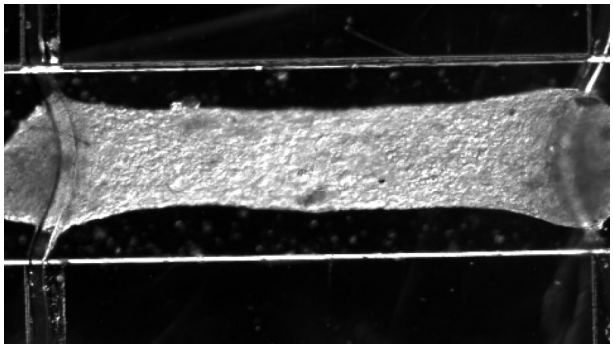

Figure 4: *Microscopic picture of the Biowire™ II Platform [18]*

4.3 Micro-spring

This is a conceptual system combining a micro-spring as used in Wang et al. 2018 [19] and a small magnet, controlling the external magnetic field generates a stretching force on the tissue (Figure 5). Here the micro-spring is used to generate stiffness in the system but also to create flexibility to allow muscles to contract. This system is proven to be workable. The design of this system is material-dependent while Young's modulus of the used material combined with the power of the magnet determines the elongation of the tissue.

Nevertheless, since the tissue elongation and the compression capacity of this system are determined by these material properties the system can be used for very specific cells. This is resulting in a less flexible system.

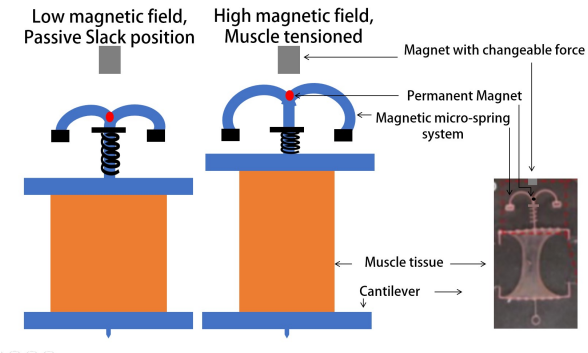

Figure 5: *Schematically representation of the conceptual micro-spring driven system*

4.4 MDirect Tensioner

This is a conceptual system combining the system based on two pillars as used in Ribeiro et al. 2022 [20] combined with a stiff PMMA pillar in a micro-screw driven slit. This construction makes it possible to culture cells between the two pillars and tension the tissue by mechanical movement of the screw-driven pillar (Figure 6). The screw in this conceptual design could also be interchanged by an air pressure-driven system. Major obstacles to this system would be the preferred size of the system, the assembly of the system and the connection between the closed air chamber of the system and the moving pillar. A plus can be that this system can be a closed solution to maintain sterility. This concept would function as an upside-down system.

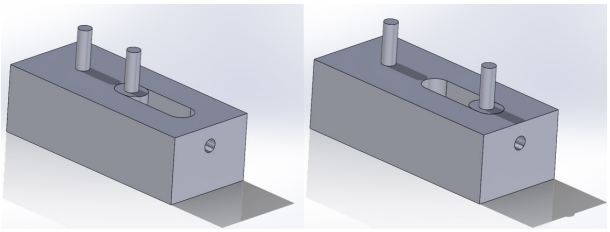

Figure 6: *Schematically representation of the conceptual Screw or air driven system*

4.5 Balloon cell tensioner

This conceptual system uses a circular muscle tissue cultured in a PDMS ring structured around a balloon. Pressurizing the balloon should stretch the tissue (Figure 7). The feasibility of this system is however unprovable, pending research towards this system is not published yet. Research that has already been performed on circular muscles aims toward stronger muscles or shorter muscles instead of elongation, the main subject here are sphincter muscles.

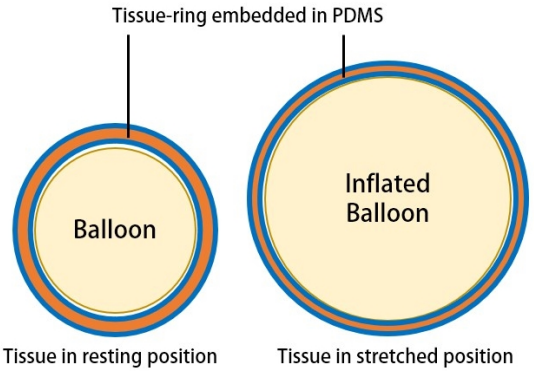

Figure 7: *Schematically representation of the conceptual Balloon driven system*

4.6 Air pressured membrane pillar deflector

In this conceptual design pillars are situated on a pressurizable membrane. Pressuring this membrane would result in an angular movement of the pillars, resulting in a bigger distance between pillar ends. This system could be used in an upright and upside-down direction. A major drawback of this system can be the flexibility of the used membrane, this flexibility limits the maximal elongation of the tissue (Figure 8).

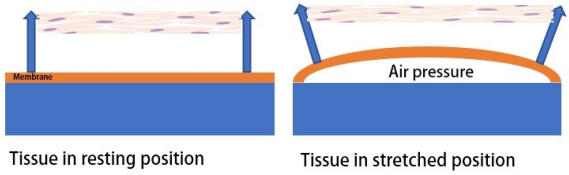

Figure 8: *Schematically representation of the conceptual air pressure driven system*

5 Prototype description

Based on the gained knowledge concerning design limitations such as complexity, workability, flexibility and feasibility following from the system and concept evaluation in chapter 4, the following decisions are made. The uBeat® and Biowire ™ II are interesting systems but not suitable for this specific research. The material-limited Micro-spring and air pressured membrane pillar deflector are very promising and possibly suitable for fulfilling the main goal of this research, but due to time and material limitations within this research this concept will not be used for the prototype. The Balloon cell tensioner is considered an interesting solution for eccentric in-vitro training but due to the absence of reference material, this concept will not be implemented in this research. Since designing a new working system from scratch, from this calibre without any reference material would be due to the limited time goal not desirable.

The chosen prototype consists of an array of pillars, where the pillar distance can be fluctuated by hydrostatic pressure.

Three main parts out of different materials will be used: PDMS pillars for interaction with the tissue, a PMMA bottom where the tissues can be cultured in a gelatin mold around the pillars and a 3D-printed top consisting of two parts that can be controlled mechanically. By controlling the pillar's distance and electro-stimulating the cells, eccentric training within this system should be possible. The design of the prototype will be based on the principle of the MDirect Tensioner as described in 2.2.4. Certain changes were made to the design to make it more feasible for rapid prototyping. All the 3D models in this paper are designed with Solidworks Education Edition 2021 (Dassault Systèmes SolidWorks Corp., Massachusetts, USA).

The main functionality of the prototype is formed by the mechanical top part, which is controllable by a hydrostatically driven syringe. This mechanical top part consists of two sliders, one of these sliders is 2 mm higher than the other one and has a protruding edge. This was designed to cover up the space that is formed by the reciprocating sliders in order to make a more closed system to overcome contamination (Figure 9 and 10). The large slider also includes 2 holes with a diameter of 2 mm for electrodes to make electro-stimulation through the medium possible.

The sliders have three oval structures hanging underneath their basis. These structures fit the PDMS sheets which are 3 mm thick. Each sheet has 6 pillars of 3.25 mm long with a diameter of 500 µm. Each pillar has a 100 µm thick disc on top with a diameter of 1 mm to prevent the cells from falling from the pillars. The pillar ends are stained black to create optical contrast compared to the tissue (Figure 11). The deflection of the pillars will be tracked using the black stained pillar tops. By measuring the amount of deflection of the pillars, the force that the muscle tissue exerts on the pillars can be calculated with the equation below [20].

$$F = \frac{3\pi E R^4}{2a^2(3L-a)}(3 \cdot 10^{-3} + \sum P_S) \tag{1}$$

With F in Newton, E is Young's modulus of the PDMS, R the radius of the pillars and L the length of the pillars. a is the distance between the tissue and the base of the PDMS sheet. P_S is the performed step distance.

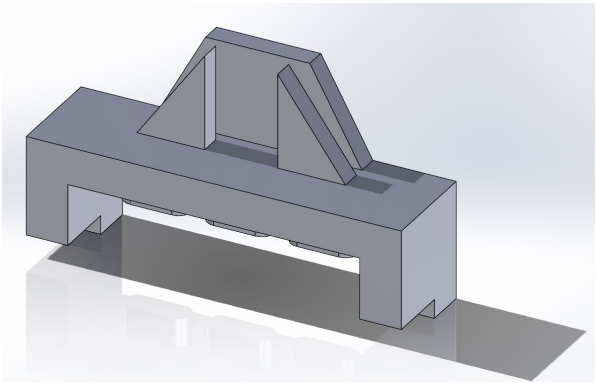

Figure 9: *Graphical representation of the small slider*

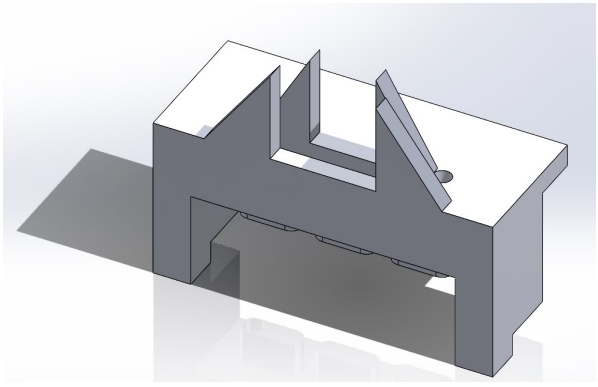

Figure 10: *Graphical representation of the large slider with protruding edge*

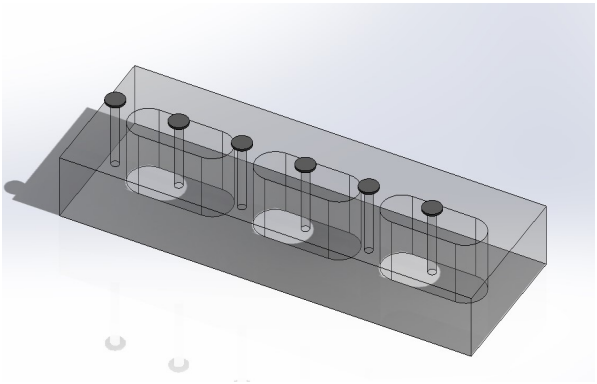

Figure 11: *Graphical representation of the needed PDMS sheet*

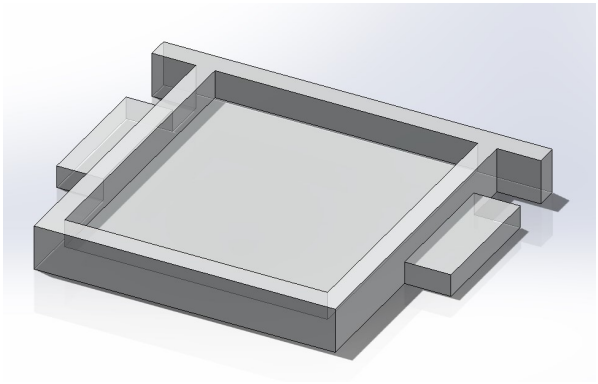

Figure 12: *Graphical representation of the bottom plate*

The sliders are guided by the bottom plate. This bottom plate is 4 mm high with a reservoir of 2.5 mm deep (Figure 12). This reservoir can be filled with cell medium or with gelatin, in the case of gelatin, the cell shape mold can be used to create the tissue slots (Figure 13). Six tissue slots can be made by the use of the mold, resulting in the possibility to test six tissues at once within this system. These slots are 1.8 mm wide and 5.8 mm long to create a mold for a maximum of $2.5 \cdot 10^5$ cells. Making use of more cells would result in a larger cross-sectional area limiting the research possibilities on a microscope. On top of the sliders triangular structures where made for tight-fitting the syringe (Figure 9 and 10).

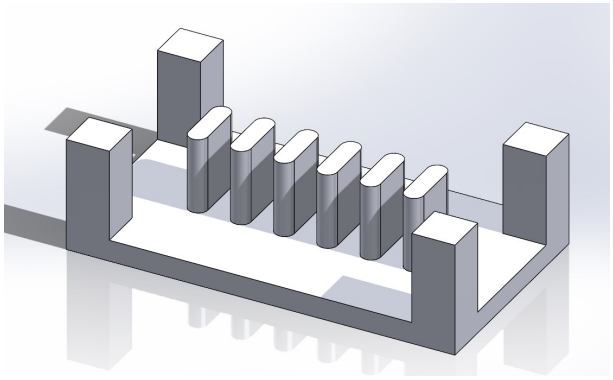

Figure 13: *Graphical representation of the cell shape mold*

This syringe is responsible for the movement of the pillars. This syringe is connected via a tube with an inner diameter of 1.27 mm to another syringe placed in a syringe pump. It is assumed that by infusing the syringe placed on the prototype the two sliders move away from each other making the internal pillar distance bigger. Withdrawal of the syringe on the prototype leads to a smaller internal pillar distance. By using the equation below, it can be calculated which volume is needed for a specific translation of the pillars.

$$V = \pi \cdot r^2 \cdot x \tag{2}$$

In the equation above, V is the volume (m^3) that has to be programmed on the syringe pump. r is the radius (m) of the syringe mounted on the prototype. x is the desired translation distance of the pillars in meters. A syringe with a diameter of 9.8 mm was used on the prototype. In addition, the syringe-pump needs programming defined in liters, this result in the following equation.

$$V = 7.543 \cdot 10^{-2} \cdot x \tag{3}$$

The system is designed to fit in a 94 mm petri-dish, a total overview of the system can be seen in figure 14 and 15.

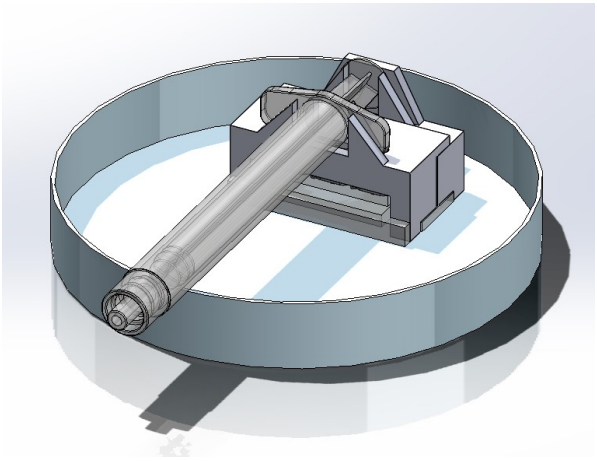

Figure 14: *Graphical representation of the prototype placed in an 94 mm petri-dish*

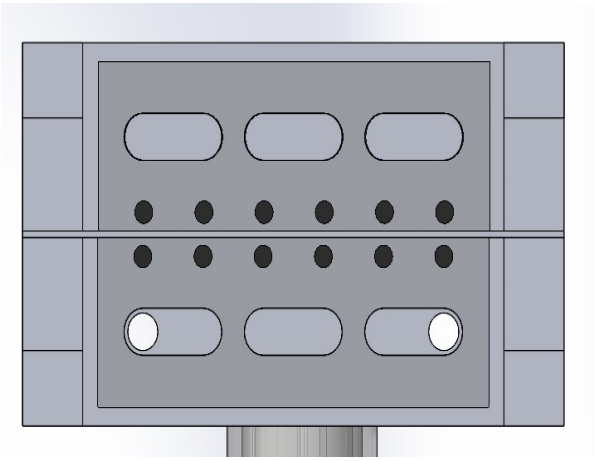

Figure 15: *Graphical representation of pillar placement on the prototype*

5.1 Fabrication

The designed system consists of different materials. The bottom plate can be made out of poly(methyl methacrylate) (PMMA). This is a thermoplastic with robust and transparent properties. PMMA is also easy to mass produce [21]. This robustness and transparency are needed for creating a robust basis which does not react with the cell medium and is usable under a conventional light microscope. PMMA can be micro-milled.

Poly(dimethylsiloxane) (PDMS) is chosen for the pillars, while PDMS is known for its silicone rubber structure, biocompatibility, optical transparency and gas permeability. PDMS can be produced in high-quality nanostructures [21]. The flexibility of the pillars is used for measuring the force exerted by the tissues as described in equation 1.

The PDMS sheets were produced by mold-casting making use of a 1:10 volume ratio of Sylgard 184 (Sigma-Aldrich, St. Louis, MO, USA) into the PDMS molds as seen in figure 16. The mold was placed in a vacuum environment for 45 minutes and cured afterwards in an incubator for 60°C overnight. After curing the tops of the pillars were marked by a mixture of PDMS and 13% weight percentage of black carbon (Vulcan XC 72R), this was cured for 2 hours on 60°C [20]. The disc mold was placed in the bottom plate and used to create the PDMS discs on top of the pillars. This was done by hanging the PDMS sheets in the prototype system, and placing the pillar ends in the disc slots (Figure 17 and 18). These discs were made of the same PDMS ratio as stated above and where cured on 60°C for 2 hours.

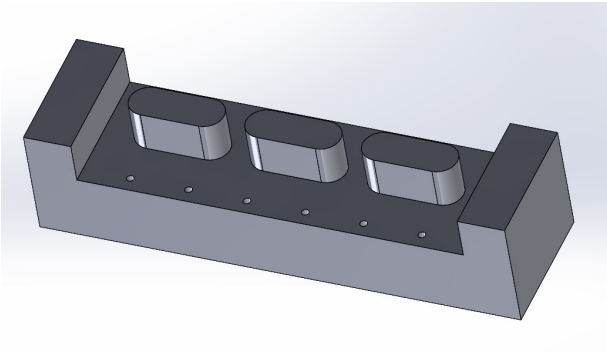

Figure 16: *Graphical representation of the PDMS sheet mold*

The sliders and molds were 3D printed, due to time limits and fast prototyping considerations the bottom plate was also 3D printed. A resin-printer (Form 3L, Formlabs, Somerville, Massachusetts, USA) was used with Tough 1500 resin (Formlabs, Somerville, Massachusetts, USA), this resin is proven bio-compatible [22]. After printing the parts were washed with IPA (2-propanol (Isopropyl alcohol)) in a Form Wash L (Formlabs, Somerville, Massachusetts, USA). When the parts were washed, they were placed in the Form Cure L (Formlabs, Somerville, Massachusetts, USA) to be cured at a temperature of 70°C by UV light. After curing, the supports

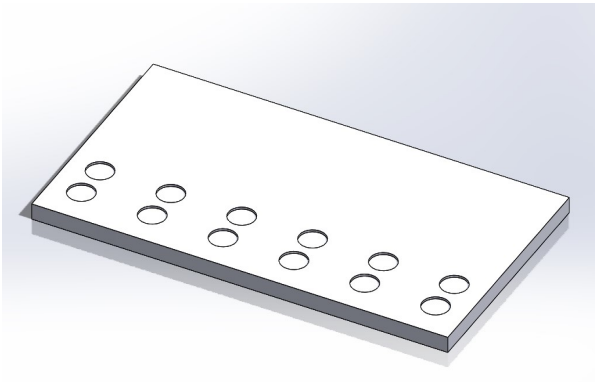

Figure 17: *Graphical representation of the Disc mold*

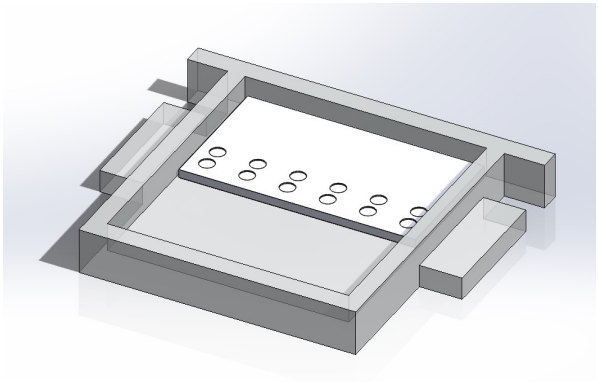

Figure 18: *Graphical representation of the disc mold placed in the bottom plate*

were removed, and the rough areas as a result of the supports were sanded with a P420 sanding paper. Afterwards, the parts were made dust-free and cleaned by pressurized air and IPA. After these steps, the chip was assembled as seen in chapter 5. Also see figure 19, 20 and 21. In figure 22 an overview of all the parts and materials can be seen. The syringe pump and disc mold were not included in this figure, the syringes, tubing and petri-dish as seen in the figure can be chosen differently. By using a syringe with another diameter than used in this research, equation 3 should be adjusted. This adjustment can be calculated by equation 2. The used materials in figure 22 will be elaborated in the subsection materials of the prototype testing section.

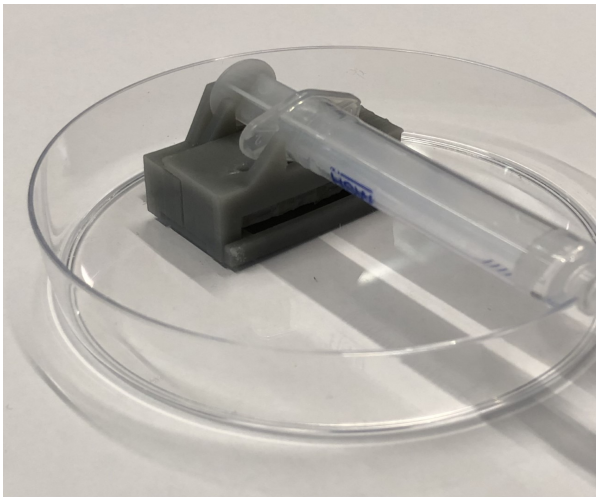

Figure 19: *Overview of the fabricated prototype*

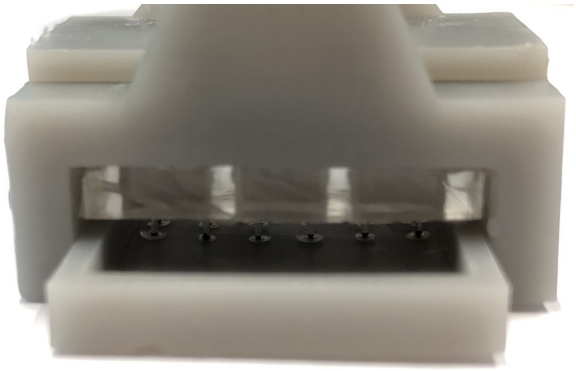

Figure 20: *Side view of the prototype focused on the pillars*

Figure 21: *Pillars placed on the prototype*

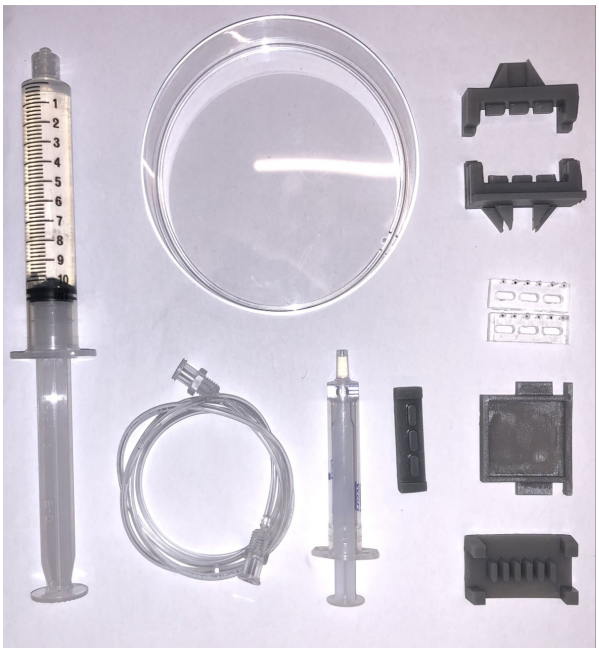

Figure 22: *Overview of all the parts and materials for assembly of the prototype*

5.2 Prototype operation

To use this system to prove eccentric training as a stimulating factor for longitudinal muscle growth, the system can be operated as followed:

Sterilize the system and assemble the system as considered in chapter 5. Fill the syringes and tubing with water or another fluid with a high bulk modulus, and prevent air within the syringe-tubing combination by filling the combination submerged into the fluid. Place the syringes on the syringe pump and the prototype. Place the system in a petri-dish to make the system more portable and contamination resistant. Fill the bottom plate with a mixture of gelatin (G1890-1006) and 1 mL of double the concentration of cell medium used for the specific cells. Use a 20% weight to volume ratio for the gelatin [20]. Place the cell shape mold on top, and put it away for 4 hours before experimenting on 4 °C.

Remove the cell shape mold and fill the tissue slots with 20 µl of cell suspension (max. $2.5 \cdot 10^5$ cells per slot). Place the PDMS pillars attached to the mechanical top part in the tissue slots. Incubate at room temperature for 10 minutes and fill the bottom plate afterwards with 1.5 ml cell medium. Maintain the cells as needed for the specific kind of chosen cells.

Perform eccentric training on the cells by changing the pillar distance as described in chapter 5 and equation 3. Stimulate the cells by placing electrodes in the predestined holes and choose a pacing protocol.

To prove eccentric training as a stimulating factor for longitudinal muscle growth, the length-force relation of the tissue should be studied. The PDMS pillars placed on the prototype have Young's modulus of 2.05 MPa. By making use of equation 1, the force of the tissue acting on the pillars can be determined. The pillar deflection can be measured by optical tracking of the distance between the black stained pillar tops using a microscope. Perform fluorescence microscopy to investigate cell orientation and properties.

5.3 Prototype testing

In this section, the prototype will be tested on work-ability and performance. This will be done by measuring the deviation between the set change in pillar distance by using the equation 3 and the performed change of pillar distance by the prototype.

5.3.1 Materials

- The prototype as described in section 5
- 2ml (3ml) syringe (HENKE-JECT, HENKE SASS WOLF, Tuttlingen, Germany)
- 10ml syringe (BD, Becton, Dickinson and Company, USA)
- Syringe pump (PHD Ultra™, Harvard apparatus, Massachusetts, USA)
- Medical tubing 1.27mm (Tygon® ND 100-80, Saint-Gobain, France)
- Tubing-Luer connectors female
- 94 mm Petri-dish (Greiner, Austria)
- Digital microscope (Dino-Lite AM7915MZTL EDGE, Dino-Lite, Netherlands)
- DinoCapture 2.0 Software (Dino-Lite, Netherlands)
- Medical tape 2.5 mm (Strappal Tape, BSN Medical, Netherlands)
- 20 ml water (H_2O)
- Elevated surface area
- Universal standard with mounting hub.

5.3.2 Method

The prototype assembled as stated in section 5 was placed without the bottom plate in the petri-dish. This was done to make the pillars underneath the prototype visible. It was assumed based on material specifications and dimensions that any friction between the sliders and the bottom plate would not influence the performance of the system. The petri-dish was fixated with medical tape to an elevated surface area. The digital microscope was mounted upside down on the universal standard and was focused on the pillars (Figure 24). The DinoCapture software was launched and coupled to the microscope by a USB 2.0 connection. The included N3C-S Cover (Dino-Lite, Netherlands) was chosen for the microscope, to create an image with more depth and texture. The syringe pump was turned on and set to the specific volumes, these volumes can be seen in table 1 as well as the used mode on the syringe pump and the magnification of the microscope.

Table 1: *Overview of the used settings for the prototype testing*

Distance x (mm)	Set volume (µl)	Syringe pump mode	Microscopic Magnification
10	738.981	Infuse	8x
10	738.981	Withdraw	8x
5	369.491	Infuse	27x
5	369.491	Withdraw	27x
1	73.898	Infuse	55x
1	73.898	Withdraw	55x
0.5	36.949	Infuse	55x
0.5	36.949	Withdraw	55x
0.1	7.3898	Infuse	55x
0.1	7.3898	Withdraw	55x

These volumes were calculated by equation 3. Every measurement series consisted of a repetition of steps. Every measurement series was done at least three times, taking into account that the used syringe on the prototype results in a theoretical minimal pillars distance of 3 mm caused by the dimensions of the sliders and the PDMS sheet. The use of this syringe resulted in a maximum of 38 mm. This maximum would be reduced by the use of the bottom plate to 12 mm. Every measurement couple consists of a series of infusion steps and a series with the same amount of steps of withdrawal. Infusion results in an increase in pillar distance, and withdrawal in a decrease of pillar distance. The pillar distance was measured before starting the experiment and after each step made by the syringe pump. Every step was performed with a speed of 220 µm/s (1 ml/min). The performed step distance was determined by the use of the measurement tool of the DinoCapture software. With this, the centres of the black stained pillars were selected and the distance between these centres was exported to Excel (Excel Microsoft 365, Microsoft, USA) (Figure 23). The measured distances were used to calculate the step distance as performed by the prototype. This was done by making use of equation below.

$$P_S = |P_D^{Final} - P_D^{Initial}| \tag{4}$$

With Pillar Distance (P_D) being the distance between the pillars on the prototype and the performed step is given by (P_S). This distance was compared to the set distance as described in table 1. The accuracy of every step was calculated by the below equation. The mean accuracy of the system was plotted against the step distance in Excel.

$$Accuracy = (1 - \frac{|x - P_S|}{x}) \cdot 100\% \tag{5}$$

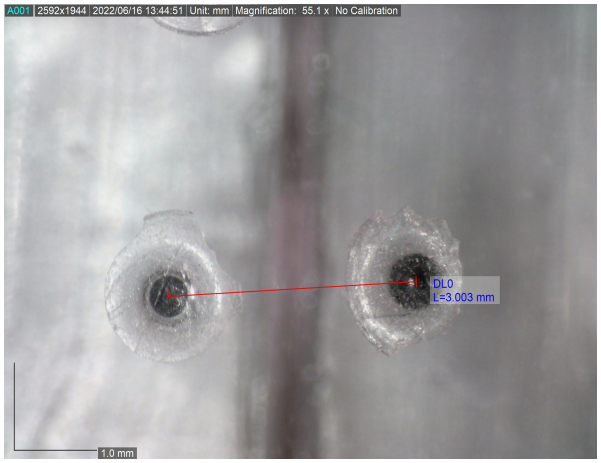

Figure 23: *Set of two pillars, measured by the DinoCapture software, magnification of 55,1x*

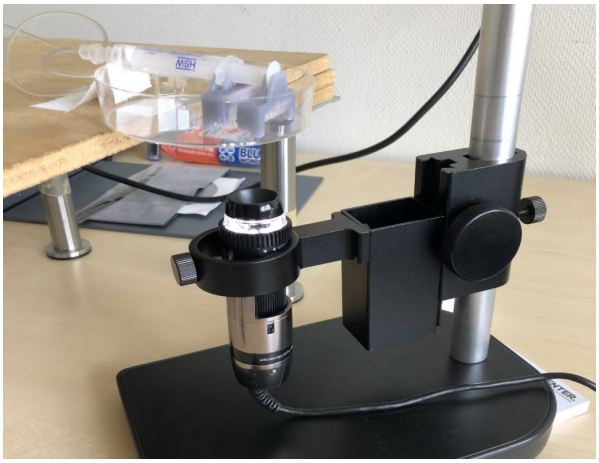

Figure 24: *The used experimental setup, syringe pump not in-captured*

5.3.3 Results

In this section, the results of the pillar distance measurements of the system are shown. Each table represents a measurement series with a specific set step distance of the syringe pump. Every step distance was determined by the final distance of the step made before the current step and the final distance after the current step. The margin of error was included for every measurement and calculation, this was based on the possible inaccuracy in the selection of the centre of the black stained pillar tops. This in-accuracy depends on the microscopic magnification. The accuracy of the syringe-pump is ± 0.25% [23] .

Table 2: *Measurements of the pillar and step distance by a 10 mm infuse syringe step, Microscopic Magnification 8x*

Step	**Final P_D (mm)**	**P_S (mm)**	**Step Accuracy (%)**
0	2.8 ± 0.1	N/A	N/A
1	9.2 ± 0.1	6.40 ± 0.14	64.0 ± 1.4
2	19.9 ± 0.1	10.66 ± 0.14	93.4 ± 1.4
3	30.1 ± 0.1	10.19 ± 0.14	98.1 ± 1.4
Mean Accuracy			85.2 ± 0.8

Table 3: *Measurements of the pillar and step distance by a 10 mm withdrawal syringe step, Microscopic Magnification 8x*

Step	**Final P_D (mm)**	**P_S (mm)**	**Step Accuracy (%)**
0	30.2 ± 0.1	N/A	N/A
1	23.5 ± 0.1	6.72 ± 0.14	67.2 ± 1.4
2	13.8 ± 0.1	9.68 ± 0.14	96.8 ± 1.4
3	3.3 ± 0.1	10.49 ± 0.14	95.1 ± 1.4
Mean Accuracy			86.4 ± 0.8

Table 4: *Measurements of the pillar and step distance by a 5 mm infuse syringe step, Microscopic Magnification 27x*

Step	Final P_D (mm)	P_S (mm)	Step Accuracy (%)
0	3.15 ± 0.03	N/A	N/A
1	4.49 ± 0.03	1.35 ± 0.04	27.0 ± 0.8
2	10.01 ± 0.03	5.52 ± 0.04	89.7 ± 0.8
3	15.16 ± 0.03	5.15 ± 0.04	97.0 ± 0.8
Mean Accuracy			71.22 ± 0.5

Table 5: *Measurements of the pillar and step distance by a 5 mm withdrawal syringe step, Microscopic Magnification 27x*

Step	Final P_D (mm)	P_S (mm)	Step Accuracy (%)
0	15.16 ± 0.03	N/A	N/A
1	13.91 ± 0.03	1.24 ± 0.04	24.9 ± 0.8
2	8.94 ± 0.03	4.98 ± 0.04	99.6 ± 0.8
3	3.23 ± 0.03	5.71 ± 0.04	85.9 ± 0.8
Mean Accuracy			70.1 ± 0.5

Table 6: *Measurements of the pillar and step distance by a 1 mm infuse syringe step, Microscopic Magnification 55x*

Step	Final P_D (mm)	P_S (mm)	Step Accuracy (%)
0	3.074 ± 0.015	N/A	N/A
1	3.507 ± 0.015	0.43 ± 0.02	43 ± 2
2	4.477 ± 0.015	0.97 ± 0.02	97 ± 2
3	5.484 ± 0.015	1.01 ± 0.02	99 ± 2
4	6.553 ± 0.015	1.07 ± 0.02	93 ± 2
Mean Accuracy			83 ± 1

Table 7: *Measurements of the pillar and step distance by a 1 mm withdrawal syringe step, Microscopic Magnification 55x*

Step	Final P_D (mm)	P_S (mm)	Step Accuracy (%)
0	5.032 ± 0.015	N/A	N/A
1	3.888 ± 0.015	1.14 ± 0.02	86 ± 2
2	3.092 ± 0.015	0.80 ± 0.02	80 ± 2
Mean Accuracy			82.6 ± 1.4

Table 8: *Measurements of the pillar and step distance by a 0.5 mm infuse syringe step, Microscopic Magnification 55x*

Step	Final P_D (mm)	P_S (mm)	Step Accuracy (%)
0	3.051 ± 0.015	N/A	N/A
1	3.207 ± 0.015	0.16 ± 0.02	31 ± 4
2	3.397 ± 0.015	0.19 ± 0.02	38 ± 4
3	3.786 ± 0.015	0.39 ± 0.02	78 ± 4
4	4.156 ± 0.015	0.37 ± 0.02	74 ± 4
5	4.453 ± 0.015	0.30 ± 0.02	59 ± 4
6	4.977 ± 0.015	0.52 ± 0.02	95 ± 4
7	5.668 ± 0.015	0.69 ± 0.02	62 ± 4
8	6.261 ± 0.015	0.59 ± 0.02	81 ± 4
Mean Accuracy			64.9 ± 1.4

Table 9: *Measurements of the pillar and step distance by a 0.5 mm withdrawal syringe step, Microscopic Magnification 55x*

Step	Final P_D (mm)	P_S (mm)	Step Accuracy (%)
0	6.034 $\pm$ 0.015	N/A	N/A
1	5.608 $\pm$ 0.015	0.43 $\pm$ 0.02	85 $\pm$ 4
2	5.457 $\pm$ 0.015	0.15 $\pm$ 0.02	30 $\pm$ 4
3	4.963 $\pm$ 0.015	0.49 $\pm$ 0.02	99 $\pm$ 4
4	4.067 $\pm$ 0.015	0.90 $\pm$ 0.02	21 $\pm$ 4
5	3.329 $\pm$ 0.015	0.74 $\pm$ 0.02	52 $\pm$ 4
6	2.946 $\pm$ 0.015	0.38 $\pm$ 0.02	77 $\pm$ 4
Mean Accuracy			61 $\pm$ 2

Table 10: *Measurements of the pillar and step distance by a 0.1 mm withdrawal syringe step, Microscopic Magnification 55x*

Step	Final P_D (mm)	P_S (mm)	Step Accuracy (%)
0	3.276 $\pm$ 0.015	N/A	N/A
1	3.268 $\pm$ 0.015	0.01 $\pm$ 0.02	8 $\pm$ 20
2	3.132 $\pm$ 0.015	0.14 $\pm$ 0.02	64 $\pm$ 20
3	3.063 $\pm$ 0.015	0.07 $\pm$ 0.02	69 $\pm$ 20
4	2.99 $\pm$ 0.015	0.07 $\pm$ 0.02	73 $\pm$ 20
Mean Accuracy			54 $\pm$ 10

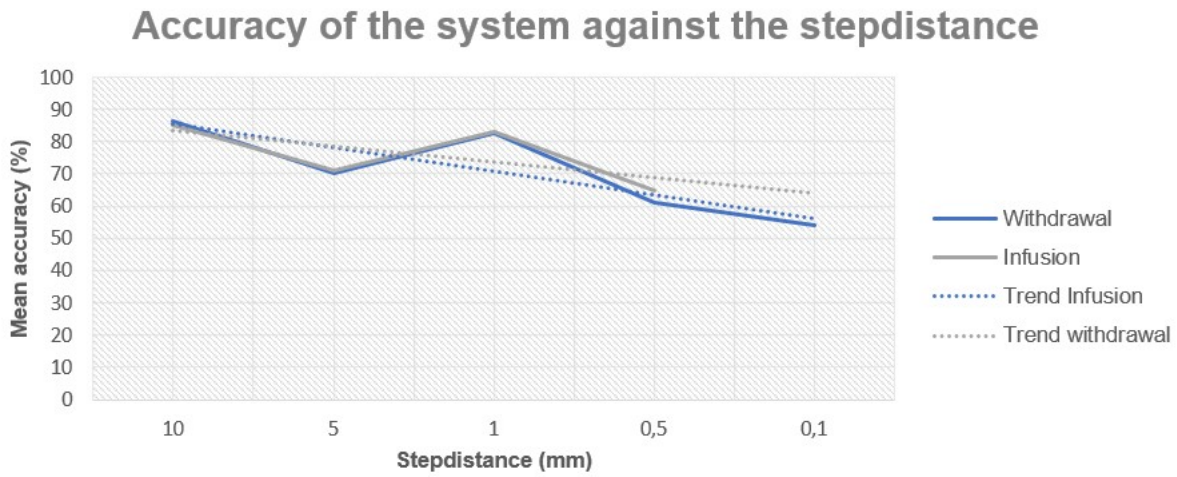

Figure 25: *The mean accuracy of the system plotted against the step distance, the margin of error was not included in the plot but has to be taken into account.*

In table 2, it can be seen that three steps were made. Step 1 lacks accuracy in comparison to the subsequent steps. Table 3 shows also three made steps, the first step lacks accuracy compared to the subsequent steps. The first step represented in table 4 lacks also in accuracy compared to the up-following steps but is considerably much more deviating from the set step distance than seen in previous first steps as mentioned above. This influences the mean accuracy. In table 5 again a very low accuracy can be seen for the first step, influencing the mean accuracy. For table 6 it can also be seen that the first step has a way lower accuracy than the subsequent steps. It can be seen that the margin of error becomes greater percentage-wise by bigger microscopic magnification. In this table, more steps than in the tables of the previous measurements are visualized, making the influence of individual steps on the mean accuracy smaller. In table 7 fewer measurements are seen than before. In this measurement series the first step has no lack in accuracy in comparison to the next step. Table 8 shows more measurements than seen in the tables of the measurements with bigger set step distances. However, the accuracy seems to be more fluctuating along with the measurement series. This influences the

mean accuracy, a lower mean accuracy is seen within this measurement series compared to the measurement series with bigger set step distances. In the measurement series visualized in table 9 big fluctuations are also seen in the step accuracy, influencing the mean accuracy. It is seen that the error margin increases by a smaller set step distance. In table 10, it is seen that in the measurement series with a 0.1 mm withdrawal step the accuracy overall can be considered as lower than seen in the measurement series with bigger set step distances. The first step has very low accuracy and the big error margin within this measurement makes it impossible to significantly state that there was a pillar movement within the first step. The margin of error for this overall measurement series is very big compared to its measured values. In figure 25 a negative trend is seen for the accuracy of the infusion steps as well for the withdrawal steps. The accuracy is comparable for the two directions.

6 Discussion

Within this research it was aimed to design a working in-vitro system to be able to prove eccentric training as a stimulus for sarcomere addition in series. It is found that a system based on hydrostatic pressure making use of syringes is most suitable within this research and time frame. It is seen that the system can perform pillar movement in two directions, initiating a smaller or greater pillar distance. A decrease in accuracy of the system is seen when the set system movement becomes smaller, no influence on the accuracy is seen from the direction of the system movement. The set requirements for this system can be met or are likely to be met by small adjustments to the system. Having a working system to prove eccentric training as a stimulus for longitudinal sacromer addition can be an important additive for research on muscular diseases. In this specific research, it proves a non-invasive alternative to improve the locomotion of patients with spasticity.

6.1 Prototype selection

To find a working system, system and concept evaluation was performed. Only one concept is chosen to be investigated and fabricated. Furthermore, some concepts were considered unsuitable based on time limitations. In this thesis a very specific time frame of 11 weeks was taken for the complete research. If time would have been a less limiting factor, it would valuable to investigate and test more different systems. The Biowire™ II Platform could be theoretically used for eccentric training if the positioning limitation is taken away, for instance by a specific wire positioning aid. Adding force measurement of the tissue within this system would make this system very promising. The Micro-spring system is considered complex, but if time is not a limiting factor proper material studies could be done to make this system workable and more flexible. The screw system within the MDirect Tensioner is comparable with the screw placed in the syringe pump. Using an screw instead of hydro-static pressure can downscale accuracy fluctuations. If this screw system would be programmable, the MDirect Tensioner with screw could be very promising. A concept like the Balloon cell tensioner which has to be designed from scratch can be very time-consuming. However, when time is not limiting, the Balloon cell tensioner sounds very promising.

The concept that is chosen to be investigated and fabricated (Figure 14) is controlled by the movement of a syringe placed on top of the prototype. Rotating of the system caused by rotation of the syringe is theoretically possible. However, this was not seen during any testing, the bottom plate also limits the possibility of rotation. In reality the used syringe on the prototype is stiff enough that rotation of the syringe is nearly impossible. Another movement that theoretically could be seen within the system is bending. This bending is defined as a movement of the ground supports towards each other. Again, since a very stiff syringe is used this is not seen. The syringe is also clamped firmly between the sliders to prevent bending. It is assumed that bending will not be initiated by the force of the tissue acting on the pillars, while this force is extremely small compared to the force exerted by the syringe pump. Any force on the system caused by the tissue is also damped by pillar deflection.

6.2 System performance

The accuracy of the movement of these sliders was measured. It was seen that the first step of the system made in the measurement series mostly lacks accuracy. It was assumed that the air within the first step is limiting, since by every first step it was seen that air travelled between the syringes before pillar movement was observed. This could be explained by leakage or air within the syringe system, caused by non-proper filling of the system and less exact syringes. It is suggested that if the system is properly filled without air within the system the accuracy of the first step would be higher, since the accuracy of the syringe pump itself does not change between steps and stays at $\pm$ 0.25% [23]. This proper filling can be done for instance by submerging the system into the fluid while filling as already recommended within 5.2 Prototype operation. The quality of the used syringe can also be a driver for leakage resulting in air within the system.

The results are suggesting that a smaller step is subject to a less accurate movement. It is assumed that this problem can also be fixed by proper filling and better syringes. However, it has to be taken into account that for a smaller step a larger magnification was used, resulting in a bigger margin of error. The margin of error within the 0.1 mm measurement seen in table 10 is considerably large that no significant statement can be made for the accuracies of this measurement series.

It is also seen that the accuracy becomes more fluctuating for smaller set steps. This would suggest that for smaller steps, the air within the system becomes more influential. Besides, within the measurement series there was tested from big towards small steps, no intermediate refilling of the syringes was done. It is assumed that

during the measurement series, the air and leakage of the system increase, resulting in a less proper filled syringe system for the small set steps than for the bigger steps. This could cause the smaller mean accuracy seen for the smaller set steps.

Where the margin of error increases along with the measurements series towards smaller set steps, the accuracy seems to decrease. This is suggested by the trend lines plotted in figure 25. However, there has to be stated that the measurement series are not consisting of the same amount of steps. This influences the mean accuracy and can result in an incorrect assumption of this accuracy. Besides, if the first steps were not to be limiting anymore the mean accuracy would increase. The fluctuation in the number of steps was caused by using the microscopic camera frame as the limit for the number of steps, steps were made as long as the pillar was seen on the camera. The 0.1 mm infuse measurement was not stated at all in the results, while the data for this measurement was not exported to Excel properly. This was detected after the measurement period, but due to the limited time frame, performing a new measurement was not possible.

During the measurement period the syringe pump stated to need lubrication, however, lubrication materials were not available during measurements. This could have influenced the performance of the syringe pump. Also, during the measurement series final pillar distances smaller than 3 mm were seen. This could be explained by small curvature in the pillars and the error margin within the selection of the centre of the pillar.

6.2.1 Requirements

Within this research it was aimed to design a system able to fulfil the main goal as stated in 2 Introduction, therefore the system was designed to be up to the requirements as stated in chapter 3. To fulfil requirement 5 the possibility to elongate the tissue is needed. It is proven that the pillars are able to move in extending direction, however, no cell tests were performed. It was aimed to perform a stretch test with cell mimicking materials. Nevertheless, this was not performed while no cell mimicking material with the right material properties was available within the short time frame. However, based on the results as described in section 5.3.3 and the fact that the Young's modulus of skeletal muscle tissue is found to be 24.7 $\pm$ 3.5 kPa [11] against the Young's modulus of 2.05 Mpa of the used PDMS pillars. It is assumed that the designed system has the theoretical potential to perform mechanical stimulation in the longitudinal direction, able to fulfill requirement 9. If the pillars do not deflect too much to tension the tissue while moving apart the system could elongate the tissue in theory by a percentage of 1167%. This makes the system up to this requirement and makes the system also suitable for other applications where more elongation than 20% is needed. To be up to requirement 10, the system should have an accuracy of at least 90%. Based on figure 25, it can be stated that the system does not fulfil this requirement. However, by preventing leakage and air within the system it is assumed that the system has the potential to be up to this requirement.

6.3 Limitations

The testing of the system as well as the research described in this thesis is limited by specific factors. One main limiting factor is the unavailability of tissue-mimicking material and tension testing, because of this the potential of the pillars to tension the tissue while moving apart can not be experimentally proved. The used stiffness is proven to be workable for cardiac muscle tissue [20]. Besides, The found Young's modulus of the muscle tissue is way lower than the Young's modulus of the used PDMS, meaning that the used PDMS is a lot stiffer than the muscle tissue. In theory, this means that if the pillars are moved apart, the tissue is more likely to be stretched than a deformation in the pillars will happen. In reality, this could result in an elongation of the tissue, while a small deformation of the pillars is seen. This would also be exactly the wanted observation for this system. However, if further research would point out that the pillars are to weak to perform the tissue tensioning, they could be adjusted by changing PDMS ratios and/or by changing pillar dimensions.

Another limitation within this research is the accuracy of the pump, it is assumed that the $\pm$ 0.25% inaccuracy of the pump would not influence the goal to prove eccentric training as a stimulus for longitudinal sarcomere addition [23]. Within the performance testing of the system, the filling of the syringe system was not performed properly up to the description as stated in section 5.2, this limited the system performance as mentioned in section 6.2.

In addition, the different steps within the performance testing were tested in at least Duplo, starting from the final pillar distance of the step made before. But, the measurement series were not repeated. This limits the significance of the measurements.

Furthermore, in the performance testing the 3D printed bottom plate was not used to make optical pillar

tracking possible. This could have influenced the performance of the system, while any possible friction between the sliders and the bottom plate was taken away by this method. However, due to material properties and the chosen dimension, it is assumed that by making use of the bottom plate no decrease in accuracy will be found. In addition, it is assumed that the force exerted by the syringe pump is big enough so that any friction between the sliders and bottom plate can be compensated.

Last, a very important limiting factor within this research is time. It was aimed to design a system up to the main goal within a period of 11 weeks. If more time would have been available, most of the points stated in this discussion section could be solved or at least further investigated.

6.4 Recommendations

For this further investigation it is recommended to perform further research into the Ballon cell tensioner, Biowire™ II Platform with wire positioning aid and the programmable screw-driven MDirect Tensioner as they sound very promising.

It is also recommended to investigate the use of more specific and higher quality syringes to prevent leakage and perform a higher precision movement. For instance with Microliter syringes [24]. It is also recommended to test the system performance when the syringes system is filled properly.

To make the performance testing more significant it is recommended to repeat the performance measurement with an equal amount of syringes steps within the measurement series, to create a more comparable mean accuracy of the step distances. To increase the significance of these measurements it is recommended to do the total performance testing at least in triplo.

However, for direct proof of concept tissue tension testing with real cells is recommended. To prove this for humans it is recommended to use for instance PCS-950-010 cells [25].

7 Conclusion

Within this research it was aimed to design an in-vitro system able to prove eccentric training as a stimulus for longitudinal muscle growth by sarcomere addition in series, to improve locomotion of patients who are suffering from spasticity. To reach this goal, a literature study was performed to collect background information about muscle behaviour, spasticity and eccentric training. A system evaluation study was performed to find the best suitable system for this research feasible within eleven weeks. It was found that a variant on the MDirect Tensioner was most feasible within this research. The designed prototype consists of a 3D printed syringe-driven system using PDMS pillars to tension and measure the force of muscle tissue. The performance of this prototype was measured.

To check if the system is able to fulfil the main goal, requirements were defined. It can be concluded that a bio-compatible system is designed, with the possibility to be kept sterile and refresh media. The system provides enough space to culture and pace tissues with a cross-sectional area of 100-200 microns, which can be investigated by fluorescence microscopy. It can be concluded that the system can mechanically stimulate tissue. The distance and force exerted by the muscle tissue can be determined. In short, it can be concluded that the system is up to the requirement 1 to 8 and 11. It is proven that in theory that the system is able to induce an elongation of muscle tissue. It is assumed that when the system is properly filled, the system would has the potential to fulfil all the formulated requirements.

It is recommended to do more performance testing of the system. Also, to proof the tissue elongation potential of the system in reality, it is recommended to perform cell testing. In short, in this thesis a prototype was designed and tested with a very high potential to be used to prove eccentric training as a stimulus for eccentric training, to improve the locomotion of patients with spasticity.

References

[1] Jeffrey S Shilt, Pennie S Seibert, and Vivek Kadyan. "Optimal management for people with severe spasticity". In: *Degenerative Neurological and Neuromuscular Disease* 2 (Oct. 2012), p. 133. DOI: 10.2147/DNND.S16630. URL: /pmc/articles/PMC6065570/%20/pmc/articles/PMC6065570/?report=abstract%20https://www.ncbi.nlm.nih.gov/pmc/articles/PMC6065570/.

[2] Cinda L. Hugos and Michelle H. Cameron. "Assessment and Measurement of Spasticity in MS: State of the Evidence". In: *Current Neurology and Neuroscience Reports 2019 19:10* 19.10 (Aug. 2019), pp. 1–7. ISSN: 1534-6293. DOI: 10.1007/S11910-019-0991-2. URL: https://link.springer.com/article/10.1007/s11910-019-0991-2.

[3] J. C. van den Noort et al. "European consensus on the concepts and measurement of the pathophysiological neuromuscular responses to passive muscle stretch". In: *European journal of neurology* 24.7 (July 2017), 981–e38. ISSN: 1468-1331. DOI: 10.1111/ENE.13322. URL: https://pubmed.ncbi.nlm.nih.gov/28557247/.

[4] Iqbal Multani et al. "Botulinum Toxin in the Management of Children with Cerebral Palsy". In: *Paediatric drugs* 21.4 (Aug. 2019), pp. 261–281. ISSN: 1179-2019. DOI: 10.1007/S40272-019-00344-8. URL: https://pubmed.ncbi.nlm.nih.gov/31257556/.

[5] Timothy J. Suchomel et al. "The Importance of Muscular Strength: Training Considerations". In: *Sports medicine (Auckland, N.Z.)* 48.4 (Apr. 2018), pp. 765–785. ISSN: 1179-2035. DOI: 10.1007/S40279-018-0862-Z. URL: https://pubmed.ncbi.nlm.nih.gov/29372481/.

[6] Elisabeth Ehler and Mathias Gautel. "The sarcomere and sarcomerogenesis". In: *Advances in experimental medicine and biology* 642 (2008), pp. 1–14. ISSN: 0065-2598. DOI: 10.1007/978-0-387-84847-1{_}1. URL: https://pubmed.ncbi.nlm.nih.gov/19181089/.

[7] B. Brenner and E. Eisenberg. "The mechanism of muscle contraction. Biochemical, mechanical, and structural approaches to elucidate cross-bridge action in muscle". In: *Basic research in cardiology* 82 Suppl 2 (1987), pp. 3–16. ISSN: 03008428. DOI: 10.1007/978-3-662-11289-2{_}1. URL: https://link.springer.com/chapter/10.1007/978-3-662-11289-2_1.

[8] Robert Arthur Elliston Seaborne. "The Role of DNA Methylation in the Regulation of Skeletal Muscle Atropy, Hypertrophy and Epigenetic Memory". In: May (2018), p. 25. DOI: 10.24377/LJMU.t.00009473. URL: http://researchonline.ljmu.ac.uk/id/eprint/9473/.

[9] Alison Cutts. "The range of sarcomere lengths in the muscles of the human lower limb." In: *Journal of Anatomy* 160 (Oct. 1988), p. 79. ISSN: 0021-8782. URL: /pmc/articles/PMC1262051/?report=abstract%20https://www.ncbi.nlm.nih.gov/pmc/articles/PMC1262051/.

[10] Dilson E. Rassier, Eun Jeong Lee, and Walter Herzog. "Modulation of passive force in single skeletal muscle fibres". In: *Biology Letters* 1.3 (Sept. 2005), p. 342. ISSN: 1744957X. DOI: 10.1098/RSBL.2005.0337. URL: /pmc/articles/PMC1617137/%20/pmc/articles/PMC1617137/?report=abstract%20https://www.ncbi.nlm.nih.gov/pmc/articles/PMC1617137/.

[11] Irina V. Ogneva, Dmitry V. Lebedev, and Boris S. Shenkman. "Transversal Stiffness and Young's Modulus of Single Fibers from Rat Soleus Muscle Probed by Atomic Force Microscopy". In: *Biophysical Journal* 98.3 (Feb. 2010), p. 418. ISSN: 15420086. DOI: 10.1016/J.BPJ.2009.10.028. URL: /pmc/articles/PMC2814213/%20/pmc/articles/PMC2814213/?report=abstract%20https://www.ncbi.nlm.nih.gov/pmc/articles/PMC2814213/.

[12] Annika Kruse et al. "Stimuli for Adaptations in Muscle Length and the Length Range of Active Force Exertion—A Narrative Review". In: *Frontiers in Physiology* 12.October (2021). ISSN: 1664042X. DOI: 10.3389/fphys.2021.742034.

[13] H.J Swatland. *Structure and Development of Meat Animals and Poultry*. Bosa Roca: Taylor & Francis Inc, 1994, pp. 396–401. ISBN: 9781566761208.

[14] Stéphanie Hody et al. "Eccentric Muscle Contractions: Risks and Benefits". In: *Frontiers in Physiology* 10.MAY (2019). ISSN: 1664042X. DOI: 10.3389/FPHYS.2019.00536. URL: /pmc/articles/PMC6510035/%20/pmc/articles/PMC6510035/?report=abstract%20https://www.ncbi.nlm.nih.gov/pmc/articles/PMC6510035/.

[15] *Products - BiomimX*. URL: https://www.biomimx.com/products/.

[16] *uBeat: the beating organs-on-chip platform — Knowledgeshare*. URL: https://www.knowledgeshare.eu/en/patent/ubeat-the-beating-organs-on-chip-platform/.

[17] *Platform – TARA / Innovating predictive cardiac physiology*. URL: https://tarabiosystems.com/platform/#.

[18] *This special platform models cardiac fibrosis - Ted Rogers Centre for Heart Research*. URL: https://tedrogersresearch.ca/2017/04/special-platform-models-cardiac-fibrosis/.

[19] Zhan Wang et al. "3D bioprinted functional and contractile cardiac tissue constructs". In: *Acta biomaterialia* 70 (Apr. 2018), pp. 48–56. ISSN: 1878-7568. DOI: 10.1016/J.ACTBIO.2018.02.007. URL: https://pubmed.ncbi.nlm.nih.gov/29452273/.

[20] Marcelo C. Ribeiro et al. "A New Versatile Platform for Assessment of Improved Cardiac Performance in Human-Engineered Heart Tissues". In: *Journal of Personalized Medicine* 12.2 (Feb. 2022), p. 214. ISSN: 20754426. DOI: 10.3390/JPM12020214/S1. URL: https://www.mdpi.com/2075-4426/12/2/214/htm%20https://www.mdpi.com/2075-4426/12/2/214.

[21] Chak Ming Leung et al. "A guide to the organ-on-a-chip". In: *Nature Reviews Methods Primers 2022 2:1* 2.1 (May 2022), pp. 1–29. ISSN: 2662-8449. DOI: 10.1038/s43586-022-00118-6. URL: https://www.nature.com/articles/s43586-022-00118-6.

[22] *Buy Tough 1500 Resin*. URL: https://formlabs.com/store/materials/tough-1500-resin/.

[23] *Standard Infuse/Withdraw PHD Ultra Syringe Pumps*. URL: https://www.harvardapparatus.com/standard-infuse-withdraw-phd-ultra-syringe-pumps.html.

[24] *Hamilton Syringes - 700 Series — Hamilton Company*. URL: https://www.hamiltoncompany.com/laboratory-products/syringes/general-syringes/microliter-syringes/700-series.

[25] *Primary Skeletal Muscle Cells — ATCC*. URL: https://www.atcc.org/products/pcs-950-010.